ISSN 0021-3640, JETP Letters, 2011, Vol. 94, No. 3, pp. 197–201. © Pleiades Publishing, Inc., 2011.
Original Russian Text © V.V. Val'kov, A.A. Golovnya, M.M. Korovushkin, 2011, published in Pis'ma v Zhurnal Eksperimental'noi i Teoreticheskoi Fiziki, 2011, Vol. 94, No. 3, pp. 215–219.

Kinematic Mechanism of the Modulation of the Spectral Intensity in the Spatially Uniform System of Hubbard Fermions

V. V. Val'kov[a, b, *], A. A. Golovnya[a, b], and M. M. Korovushkin[a, b]

[a] *Kirensky Institute of Physics, Siberian Branch, Russian Academy of Sciences, Akademgorodok, Krasnoyarsk, 660036 Russia*

[b] *Reshetnev Siberian State Aerospace University, Krasnoyarsk, 660014 Russia*

* *e-mail: vvv@iph.krasn.ru*

Received February 22, 2011; in final form, May 30, 2011

Using the exact representation of the Green's function constructed in terms of the Hubbard operators, it has been shown that the kinematic interaction that induces the spin-fluctuation processes in the spatially uniform system of Hubbard fermions leads to significant variations in the spectral intensity $A(\mathbf{k}, \omega)$ in the Brillouin zone. As a result, the modulation of $A(\mathbf{k}, \omega)$ appears in the Fermi contour. The sign of the hopping integral within the first coordination sphere is determined by the contour section, where $A(\mathbf{k}, \omega)$ decreases according to the angle-resolved photoemission spectroscopy data.

DOI: 10.1134/S0021364011150148

1. The research of cuprate superconductors have demonstrated a dominant role of strong electron correlations determining the physical characteristics of these materials. In the theoretical analysis of systems with strong electron correlations, the Hubbard model is commonly taken as the basic model [1]. In the limit of infinitely strong on-site Coulomb repulsion, the relation between the electron and spin degrees of freedom manifests via the kinematic interaction [2] and underlies the spin-fluctuation processes [3]. Later, it was found that scattering by spin fluctuations is important for the correct description of the pseudogap state in the normal phase [4]. In this situation, the interaction of electrons with a spin density wave was often considered to be a specific mechanism of spin–electron coupling.

In these studies, the existence of the spin density wave was assumed to be a postulated property and the cause of its formation was not discussed. Therefore, it is topical to analyze the mechanism underlying the formation of the pseudogap state in a spatially uniform system. In this work, the formulated problem is solved using the diagram technique for the Hubbard operators [2, 8], which makes it possible to adequately describe the main features of an ensemble of Hubbard fermions. This approach significantly involves the exact representation of the Matsubara Green's function in terms of the mass and force operators. This representation makes it possible to find the picture of fluctuating spectral intensity that agrees well with the angle-resolved photoemission spectroscopy (ARPES) data.

2. In the strong correlation regime ($U \gg t$), it is well known that the processes involving throwing electrons to the upper Hubbard subband give rise to an exchange coupling between electrons. As a result, the Hamiltonian of the system at the subspace without the states with two electrons at one site and taking into account this exchange coupling can be expressed in the form (t–J model) [9]

$$\hat{H} = \sum_{f\sigma}(\varepsilon - \mu)X_f^{\sigma\sigma} + \sum_{fm\sigma} t_{fm} X_f^{\sigma 0} X_m^{0\sigma} + \frac{1}{2}\sum_{fm} J_{fm}(X_f^{\sigma\bar{\sigma}} X_m^{\bar{\sigma}\sigma} - X_f^{\sigma\sigma} X_m^{\bar{\sigma}\bar{\sigma}}), \quad (1)$$

where $X_f^{pq} = |f, p\rangle\langle f, q|$ are the Hubbard operators [1] that describe the transition of an ion from the single-site state $|q\rangle$ to the $|p\rangle$ state, ε is the energy of the one-electron single-ion states, μ is the chemical potential of the system, $\sigma = \pm 1/2$ ($\bar{\sigma} = -\sigma$) is the spin projection, t_{fm} is the hopping integral for the electron transfer between sites m and f, $J_{fm} = 2t_{fm}^2/U$ is the exchange integral, and U is the Hubbard parameter of the on-site electron repulsion.

For calculations of the spectral intensity $A(\mathbf{k}, \omega)$, we use the diagram technique for the Hubbard operators [2, 8] and introduce the Matsubara Green's function

$$D_{0\sigma,0\sigma}(f, \tau; f', \tau') = -\langle T_\tau \tilde{X}_f^{0\sigma}(\tau)\tilde{X}_{f'}^{\sigma 0}(\tau')\rangle = \frac{T}{N}\sum_{\mathbf{k}\omega_n} e^{i\mathbf{k}(f-f') - i\omega_n(\tau-\tau')} D_{0\sigma,0\sigma}(\mathbf{k}, i\omega_n). \quad (2)$$

In the paramagnetic phase, the Green's function is independent of the spin polarization and we omit the spin subscripts. Further on, it is important that $D(\mathbf{k}, i\omega_n)$ can be factorized into a product of the propagator part and force operator [2]

$$D(\mathbf{k}, i\omega_n) = G(\mathbf{k}, i\omega_n)P(\mathbf{k}, i\omega_n). \quad (3)$$

It is easy to derive the modified Dyson equation for $G(\mathbf{k}, i\omega_n)$.

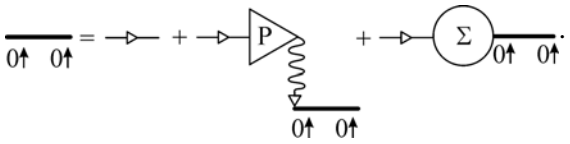

(4)

In this equation, the bold line corresponds to the full propagator $G(\mathbf{k}, i\omega_n)$ and the triangle with symbol P is the force operator $P(\mathbf{k}, i\omega_n)$. The irreducible (according to Larkin [10]) mass operator $\Sigma(\mathbf{k}, i\omega_n)$ is denoted by a circle with symbol Σ inside it. The thin line with the light (or dark) arrow denotes the bare Green's function for the Hubbard fermions, which corresponds to the explicit expression

$$G_0(i\omega_n) = \frac{1}{i\omega_m - \varepsilon + \mu}.$$

Wavy lines with light and dark arrows correspond to the Fourier transform $t_\mathbf{k}$ of the hopping integral. The relation of the full propagator and the force and mass operators can be written as [8, 11]

$$G(\mathbf{k}, i\omega_n) = \frac{1}{i\omega_m - \xi - t_\mathbf{k}P(\mathbf{k}, i\omega_n) - \Sigma^L(\mathbf{k}, i\omega_n)}, \quad (5)$$

where $\xi = \varepsilon - \mu$. Performing the analytic continuation $i\omega_n \longrightarrow \omega + i\delta$ and introducing the real and imaginary parts of the force and mass operators

$$P(\mathbf{k}, i\omega_n) \longrightarrow P(\mathbf{k}, \omega + i\delta) = P_1(\mathbf{k}, \omega) + iP_2(\mathbf{k}, \omega),$$
$$\Sigma^L(\mathbf{k}, i\omega_n) \longrightarrow \Sigma^L(\mathbf{k}, \omega + i\delta) \quad (6)$$
$$= \Sigma_1^L(\mathbf{k}, \omega) + i\Sigma_2^L(\mathbf{k}, \omega),$$

we find

$$D(\mathbf{k}, \omega + i\delta) = \frac{P_1(\mathbf{k}, \omega) + iP_2(\mathbf{k}, \omega)}{\omega - \xi - \Sigma_1^D(\mathbf{k}, \omega) + i[\delta - \Sigma_2^D(\mathbf{k}, \omega)]}. \quad (7)$$

Here,

$$\Sigma_1^D(\mathbf{k}, \omega) = t_\mathbf{k}P_1(\mathbf{k}, \omega) + \Sigma_1^L(\mathbf{k}, \omega),$$
$$\Sigma_2^D(\mathbf{k}, \omega) = t_\mathbf{k}P_2(\mathbf{k}, \omega) + \Sigma_2^L(\mathbf{k}, \omega) \quad (8)$$

are the real and imaginary parts, respectively, of the irreducible (according Dyson) mass operator. Using representation (7) for the retarded Green's function, we find the spectral intensity

$$A(\mathbf{k}, \omega) = -\frac{1}{\pi}\mathrm{Im}D(\mathbf{k}, \omega)$$
$$= -\frac{1}{\pi}\left\{\frac{[\omega - \xi - \Sigma_1^L(\mathbf{k}, \omega)]P_2(\mathbf{k}, \omega)}{[\omega - \xi - \Sigma_1^D(\mathbf{k}, \omega)]^2 + [\delta - \Sigma_2^D(\mathbf{k}, \omega)]^2}\right. \quad (9)$$
$$\left. - \frac{[\delta - \Sigma_2^L(\mathbf{k}, \omega)]P_1(\mathbf{k}, \omega)}{[\omega - \xi - \Sigma_1^D(\mathbf{k}, \omega)]^2 + [\delta - \Sigma_2^D(\mathbf{k}, \omega)]^2}\right\}.$$

The derived formula provides a solution of the formulated problem, i.e., a relation of the spectral intensity $A(\mathbf{k}, \omega)$ to the force operator $P(\mathbf{k}, \omega)$ and mass operator $\Sigma(\mathbf{k}, \omega)$. Note that the denominator in Eq. (9) includes the Dyson mass operator, whereas the numerator includes only the part of this operator that is irreducible according to Larkin. This occurs since the terms in the numerator that form the product $P_1(\mathbf{k}, \omega)P_2(\mathbf{k}, \omega)$ cancel out. Therefore, the equations for the isoenergetic surfaces (or lines in the two-dimensional case) in the crystal momentum space differ from the equations determining the surfaces with a constant value of $A(\mathbf{k}, \omega)$. This leads to the dependence of the spectral intensity on the crystal momentum on the Fermi surface. This dependence of the spectral intensity is associated with the pseudogap state of the normal phase in strongly correlated electron systems.

In the one-loop approximation [2, 8], the correction to $P(\mathbf{k}, i\omega_m)$ resulting from the interactions included to the t–J model is given by the four graphs

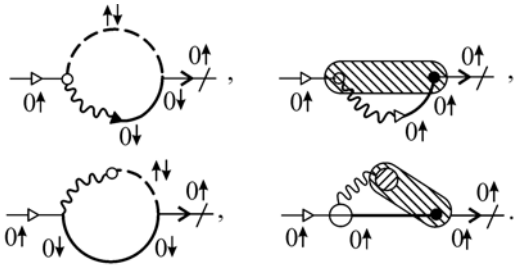

(10)

The contribution to the mass operator is determined by the two graphs

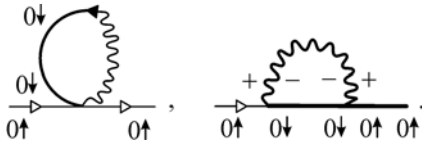

(11)

Representing the graphs in the form of analytical expressions, it is easy to obtain the force and mass operators in the form

$$P(\mathbf{k}, i\omega_m) = C_n + \frac{T}{N}\sum_{\mathbf{q}, i\omega_l}(t_\mathbf{q} + J_{\mathbf{k}-\mathbf{q}})G(\mathbf{q}, i\omega_l) \times \chi(\mathbf{q}-\mathbf{k}, i\omega_l - i\omega_m), \quad (12)$$

$$\Sigma^L(\mathbf{k}) = -\frac{T}{N}\sum_{\mathbf{q}, i\omega_l}(t_\mathbf{q} + J_{\mathbf{k}-\mathbf{q}})G(\mathbf{q}, i\omega_l), \quad (13)$$

where $C_n = 1 - n/2$ is the Hubbard renormalization.

Taking into account the expression for the Green's function $G(\mathbf{q}, i\omega_l)$, we can demonstrate that the solution of the equation for the force operator strongly depends on the form of the spin-charge susceptibility

$$\chi(\mathbf{q}, i\omega_m) = \chi_{SF}(\mathbf{q}, i\omega_m) + \chi_{CF}(\mathbf{q}, i\omega_m), \quad (14)$$

which determines the contribution of fluctuation processes. The energy scale for the charge excitations is relatively large; for this reason, we consider below only the contributions related to spin fluctuations. In this case, the nonlinear integral equation for the one-loop correction $\delta P(\mathbf{k}, i\omega_m) = P(\mathbf{k}, i\omega_m) - C_n$ to the force operator should have the form

$$\delta P(\mathbf{k}, i\omega_m) = \frac{T}{N}\sum_{\mathbf{q}, i\omega_l}\frac{(t_\mathbf{q} + J_{\mathbf{k}-\mathbf{q}})\chi_{SF}(\mathbf{q}-\mathbf{k}, i\omega_l - i\omega_m)}{i\omega_l - \xi_\mathbf{q} - t_\mathbf{q}\delta P(\mathbf{q}, i\omega_m) - \Sigma^L(\mathbf{k})}, \quad (15)$$

where $\xi_\mathbf{q} = \varepsilon + C_n t_\mathbf{q} - \mu$.

3. Since the kernel of the integral equation is determined by the dynamic magnetic susceptibility, we briefly analyze this function. For the Hubbard model, $\chi_{SF}(\mathbf{q}, \omega_m)$ was first calculated in [12]. Later on, $\chi_{SF}(\mathbf{q}, \omega_m)$ was calculated in [8, 13–15] in the context of the active research in the field of high-T_c superconductivity. The results of these calculations demonstrate that $\chi_{SF}(\mathbf{q}, \omega_m)$ deceases rapidly with an increase in the Matsubara frequency. Therefore, the main contribution to the integral equation comes from the summation over the range of ω_l in the vicinity of ω_m. Thus, we can assume that

$$\chi_{SF}(\mathbf{q}, i\omega_m) = \chi(\mathbf{q})\bar{n}_{SF}\delta_{m0}. \quad (16)$$

The function $\chi(\mathbf{q})$ is treated as the spin susceptibility at zero Matsubara frequency and $\bar{n}_{SF} \sim \Omega_{SF}/T$, where Ω_{SF} is characteristic Matsubara frequency corresponding to the onset of a steep decay of the susceptibility. The order of magnitude of this frequency is determined by the characteristic values of excitation energies in the spin subsystem, $\Omega_{SF} \sim 0.01|t|$.

For further analysis, it is important that, in the low-doping range, the $\chi(\mathbf{q})$ dependence for the t–J model exhibits a pronounced peak near the antiferromagnetic instability point $\mathbf{Q} = (\pi, \pi)$. In Fig. 1, the dashed line denotes the $\chi(\mathbf{q})$ curve calculated numerically using the technique reported in [14]. This theoretical result agrees well with the available experimental data [16]. To accelerate the numerical solution of integral equation (15), we use the model susceptibility [17, 18]

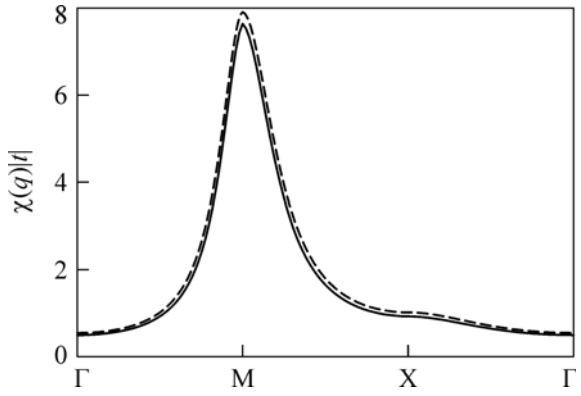

Fig. 1. Crystal momentum dependence of the susceptibility (dashed line) calculated for the t–J model [14] as compared to (solid line) the model susceptibility given by Eq. (17) determined by the numerical calculations [17, 18]. The direction of bypassing the Brillouin zone is as follows: $\Gamma(0, 0) \longrightarrow M(\pi, \pi) \longrightarrow X(\pi, 0) \longrightarrow \Gamma(0, 0)$; $J = 0.35|t|$.

$$\chi(\mathbf{q}) = \frac{\chi_0(\xi)}{1 + \xi^2(1 + \gamma_{1\mathbf{q}})}, \quad (17)$$

where

$$\chi_0(\xi) = \frac{3n}{4\omega_s C(\xi)}, \quad \omega_s = 0.55|t|, \quad \xi = 2.7,$$
$$C(\xi) = \frac{1}{N}\sum_\mathbf{q}\frac{1}{1 + \xi^2(1 + \gamma_{1\mathbf{q}})}, \quad \gamma_{1\mathbf{q}} = \frac{\cos q_x + \cos q_y}{2}. \quad (18)$$

The validity of this approximation is illustrated in Fig. 1 (the dashed line coincides with the solid line calculated using expression (17)).

Taking into account all of the aforementioned assumptions, in the first Born approximation, we find

$$\delta P(\mathbf{k}, i\omega_m) = \frac{1}{N}\sum_\mathbf{q}\frac{(t_\mathbf{q} + J_{\mathbf{k}-\mathbf{q}})\chi(\mathbf{q}-\mathbf{k})\Omega_{SF}}{i\omega_m - \xi_\mathbf{q}}, \quad (19)$$

$$\Sigma(\mathbf{k}) = -\frac{1}{N}\sum_\mathbf{q}(t_\mathbf{q} + J_{\mathbf{k}-\mathbf{q}})n_F(\xi_\mathbf{q}), \quad (20)$$

where $n_F(x) = \left[\exp\left(\frac{x-\mu}{T}\right) + 1\right]^{-1}$ is the Fermi–Dirac function. Then, the expression for the one-particle

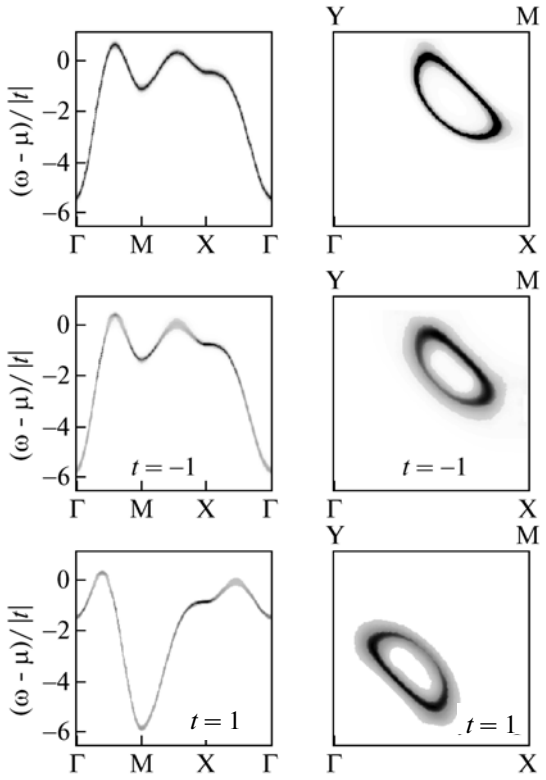

Fig. 2. Fermi excitation curves and Fermi surfaces obtained taking into account the spectral intensity. The upper panel corresponds to the Hubbard I approximation and the middle and lower panels correspond to the calculations involving the spin fluctuations with different signs of hopping integral t.

Green's function (3) has the form

$$D(\mathbf{k}, i\omega_m) = \frac{C_n + \delta P(\mathbf{k}, i\omega_m)}{i\omega_m - \xi_{\mathbf{k}} - t_{\mathbf{k}}\delta P(\mathbf{k}, i\omega_m) - \Sigma(\mathbf{k})}. \quad (21)$$

To supplement the derived set of equations, we add the following equation determining the chemical potential μ:

$$\frac{n}{2} = \frac{T}{N}\sum_{k,\,\omega_m} e^{i\omega_m\delta} D(\mathbf{k}, i\omega_m), \quad \delta \longrightarrow \infty. \quad (22)$$

The spectral intensity of the system can be calculated using the analytical continuation of Eq. (9).

4. Figure 2 shows the spectral intensity $A(\mathbf{k}, \omega)$ for the model under study calculated for (left panels) the main directions of the Brillouin zone at the electron density $n = 0.95$ and (right panels) the Fermi contours for a quarter of the Brillouin zone. The spectral intensity is presented by the intensity of lines corresponding to the energy spectrum (the darker is the line, the larger is the value of $A(\mathbf{k}, \omega)$). The model parameters in the units of $|t|$

$$T = 0.01,\ t = -1,\ t' = -0.65,\ t'' = -0.5,\ J = 0.35$$

were chosen such that the Femi surface has the shape of pockets according to the experimental data on magnetic oscillations [19]. The upper panels of Fig. 2 show $A(\mathbf{k}, \omega)$ corresponding to the Hubbard I approximation. In this case, the value of $A(\mathbf{k}, \omega)$ remains unchanged when the crystal momentum varies along the energy spectrum as well as over the Fermi surface. The middle panels show $A(\mathbf{k}, \omega)$ calculated including spin fluctuations. The comparison with the upper panel indicates that spin fluctuations lead to the qualitative difference manifesting in a pronounced modulation of $A(\mathbf{k}, \omega)$ both in the spectral lines and at the Fermi level. We can see that the most significant decrease in the value of $A(\mathbf{k}, \omega)$ occurs in a broad energy range in the vicinity of the chemical potential.

There is an important feature related to the effect of the sign of t on the behavior of the spectral intensity modulation. To demonstrate this feature, the spectral intensity calculated at the positive sign of t is presented in the lower panel of Fig. 2. In the course of the calculations, all other parameters remained fixed. We can see that, at negative t (middle panel), the spectral intensity peak appears at the Fermi contour near the (π, π) point. In the case of $t > 0$ (bottom panel), the $A(\mathbf{k}, \omega)$ peak at the Fermi contour is situated at the opposite side of the pocket, namely at the part of the contour located near the (0, 0) point. Note that this case corresponds to the results of the ARPES experiments (see, e.g., [20]).

The discussed modification of the spectral intensity related to the fluctuation processes leads to the qualitative changes in the electron density of states

$$g(\omega) = \frac{1}{N}\sum_{\mathbf{k}} A(\mathbf{k}, \omega). \quad (23)$$

Figure 3 shows the densities of states calculated (dashed line) in the Hubbard I approximation and (solid line) taking into account spin fluctuations. Comparing these two lines, we see that the fluctuation processes result in a pronounced decrease in the density of states near the chemical potential. Thus, our analysis suggests the formation of the pseudogap state in the system of Hubbard fermions under discussion.

5. In conclusion, let us emphasize the basic concepts of the discussed mechanism for the modulation of the spectral intensity $A(\mathbf{k}, \omega)$. The exact representation of the one-fermion Matsubara Green's function $D(\mathbf{k}, i\omega_m)$ is of fundamental importance [2]. The force operator in the numerator of the Green's function and its dependence on the Matsubara frequency and crystal momentum lead to the difference between the isoenergetic lines in the crystal momentum and the lines in which the force operator is fixed. This discrepancy of the isoenergetic lines and the lines corresponding to a constant value of the force operator is a cause of the $A(\mathbf{k}, \omega)$ modulation at the Fermi contour.

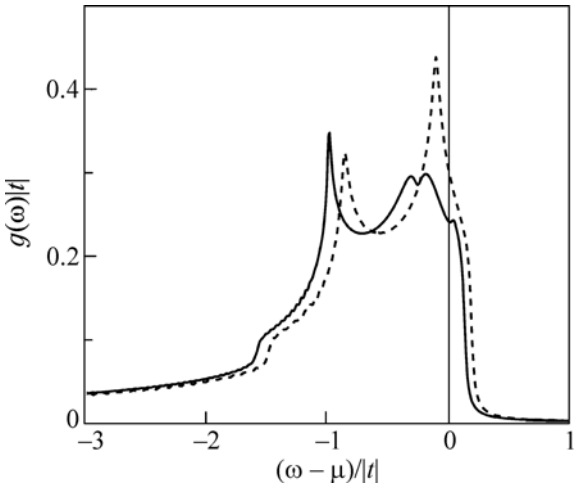

Fig. 3. Electron density of states calculated (dashed line) in the Hubbard I approximation and (solid line) taking into account the spin-fluctuation processes. The vertical straight line indicates the position of the chemical potential.

This causes also the decrease in the density of states in the vicinity of the chemical potential.

Let us also emphasize that the sign of the hopping integral t in the first coordination sphere is determined by the part of the Fermi contour that exhibits a significant decrease in $A(\mathbf{k}, \omega)$. It is clear that the revealed mechanism favoring the formation of the pseudogap phase is quite universal and should manifest itself in other models of strongly correlated electron systems.

We are grateful to R.O. Zaitsev and N.M. Plakida for the constructive criticism and helpful discussions. This work was supported by the Presidium of the Russian Academy of Sciences (program "Quantum Physics of Condensed Matter"), the Russian Foundation for Basic Research (project no. 09-02-00127), the Ministry of Education and Science of the Russian Federation (federal program "Scientific and Pedagogical Personnel of Innovative Russia" for 2009–2013), and the Siberian Branch, the Russian Academy of Sciences (integration project no. 53). The work of A.A.G. and M.M.K. was also supported by the Council of the President of the Russian Federation for Support of Young Scientists and Leading Scientific Schools (grant no. MK-1300-2011.2) and by the Siberian Branch, Russian Academy of Sciences (Lavrent'ev Competition).

REFERENCES

1. J. C. Hubbard, Proc. R. Soc. London A **276**, 238 (1963).
2. R. O. Zaitsev, Sov. Phys. JETP **41**, 100 (1975).
3. R. O. Zaitsev, J. Exp. Theor. Phys. **98**, 780 (2004).
4. M. V. Sadovskii, Phys. Usp. **44**, 515 (2001).
5. I. Eremin, M. Eremin, S. Varlamov, et al., Phys. Rev. B **56**, 11305 (1997).
6. M. V. Sadovskii, I. A. Nekrasov, E. Z. Kuchinskii, et al., Phys. Rev. B **72**, 155105 (2005).
7. N. Harrison, R. D. McDonald, and J. Singleton, Phys. Rev. Lett. **99**, 206406 (2007).
8. R. O. Zaitsev, *Diagrammatic Methods in the Theory of Superconductivity and Ferromagnetism* (Editorial URSS, Moscow, 2004) [in Russian].
9. Yu. A. Izyumov, Phys. Usp. **40**, 445 (1997).
10. V. G. Bar'yakhtar, V. E. Krivoruchko, and D. A. Yablonskii, *Green's Functions in Magnetism Theory* (Naukova Dumka, Kiev, 1984) [in Russian].
11. V. V. Val'kov and S. G. Ovchinnikov, *Quasiparticles in Strongly Correlated Systems* (Siberian Branch of RAS, Novosibirsk, 2001) [in Russian].
12. J. Hubbard and K. P. Jain, J. Phys. C (Proc. Phys. Soc.) **1**, 1650 (1968).
13. H. Shimahara and S. Takada, J. Phys. Soc. Jpn. **61**, 989 (1992).
14. A. A. Vladimirov, D. Ile, and N. M. Plakida, Theor. Math. Phys. **152**, 538 (2007).
15. M. V. Eremin, A. A. Aleev, and I. M. Eremin, J. Exp. Theor. Phys. **106**, 752 (2008).
16. P. C. Hammel, M. Takigawa, R. H. Heffner, et al., Phys. Rev. Lett. **63**, 1992 (1989).
17. N. M. Plakida, L. Anton, S. Adam, and G. Adam, J. Exp. Theor. Phys. **97**, 331 (2003).
18. J. Jaklic and P. Prelovšek, Phys. Rev. Lett. **74**, 3411 (1995); Phys. Rev. Lett. **75**, 1340 (1995).
19. N. Doiron-Leyraud, C. Proust, D. Le Boeuf, et al., Nature **447**, 565 (2007).
20. M. Hashimoto, T. Yoshida, H. Yagi, et al., Phys. Rev. B **77**, 094516 (2008).

Translated by K. Kugel